Acta Otolaryngol (Stockh) 1989; Suppl. 467: 257–264

CHAPTER 31

Models of Nonlinear Vibration. III. Oscillator with Bilinear Mass

SUZANNE E. KEILSON,[1] MALVIN C. TEICH[1] and SHYAM M. KHANNA[2]

Columbia University, Departments of [1]Applied Physics and [2]Otolaryngology, New York, USA

INTRODUCTION

In previous papers we introduced the bilinear resistance oscillator and the bilinear stiffness oscillator (Keilson, Teich and Khanna, 1989; Teich, Keilson and Khanna, 1989). In this paper we continue our investigation into the behavior of bilinear oscillators with a study of the bilinear mass oscillator. The general approach and numerical methods used to study such dynamical systems were described in Keilson, Teich and Khanna (1989), and have been considered in other references in the field of nonlinear dynamics (Thompson and Stewart, 1986; Berge, Pomeau and Christian, 1986). The bilinear mass oscillator exhibits a mass with value m_1 when the displacement is positive with respect to an arbitrary origin and m_2 when it is negative with respect to that origin. Such simple deterministic systems have enough degrees of freedom to exhibit complex behavior, such as subharmonic resonances and chaotic motion.

THEORY

The equation of motion of a bilinear mass oscillator is

$$m(x)\,x''(t)+rx'(t)+kx(t) = A_o\cos(2\pi f_s t), \tag{1}$$

where x, x′, and x″ represent the displacement, velocity, and acceleration, respectively, and the coefficients m, r, and k represent the mass, resistance, and stiffness respectively. This is an ordinary, nonlinear, nonautonomous differential equation since the mass coefficient m(x) is a function of the displacement x and the time t appears as an explicit variable in the forcing function. The forcing function has an amplitude A_o and a frequency f_s. For the bilinear mass oscillator,

$$\begin{aligned} m(x) &= m_1 \quad \text{for } x \geqslant 0 \\ m(x) &= m_2 \quad \text{for } x < 0. \end{aligned} \tag{2}$$

As a result of the form of Eq. (2), the solution scales linearly with the amplitude of the forcing function A_o so that the normalized displacement and velocity, and their spectra, do not change with the applied signal level. For the case of arbitrary m(x) the solution does not in general scale linearly with A_o so that the results will depend on the amplitude of the forcing function. When the values of the two masses differ only slightly, the deviations of the displacement and velocity waveforms from sinusoidal behavior are small. This oscillator acts as a tuned circuit with a resonance or best frequency (CF), but with harmonic content that changes as a function of the forcing (signal) frequency in a complex way.

Dividing Eq. (1) by m(x) in Eq. (2) leads to

$$x''(t)+r_i\,x'(t)+k_i\,x(t) = A_i\cos(2\pi f_s t), \tag{3}$$

where $r_i=r/m_i$, $k_i=k/m_i$, $A_i=A_o/m_i$, and where the m_i's are the two different mass constants in the two displacement domains. This demonstrates that the bilinear mass oscillator contains elements of bilinear stiffness and bilinear resistance, but in this interpretation the forcing function is also bilinear. Not surprisingly, the solutions exhibit some of the features of both the bilinear resistance and bilinear stiffness oscillators examined earlier (Keilson, Teich and Khanna, 1989; Teich, Keilson and Khanna, 1989).

Results are shown in the form of displacement waveforms and their Fourier spectra, velocity waveforms and their spectra, phase-space projections, and plots of the velocity harmonics as a function of signal frequency. The integration was always started with the initial conditions $x(0)=x'(0)=0$. Startup transients were removed by first integrating for 10,000 steps before storing the solutions. The time course of the stored solution was sufficiently long so that convergence to a limiting motion could usually be observed empirically. The spectra were obtained by a fast-Fourier transform (FFT) operation on the discrete array containing the sampled time waveform.

RESULTS

Solutions for the sinusoidally forced bilinear mass oscillator were obtained by using the values $A_o=100$ dynes, $m_1=1\times10^{-6}$ g, $m_2=1\times10^{-5}$ g, $k=16$ dyne/cm, and $r=0.005$ dyne-sec/cm in Eqs. (1) and (2). The solutions presented are representative and not peculiar to this choice of parameters. The best frequency (CF) of this oscillator is given approximately by $k^{1/2}\pi(m_1^{1/2}+m_2^{1/2})=317$ Hz. This was chosen to be the same as the best frequency of the bilinear resistance oscillator (Keilson, Teich and Khanna, 1989) and the bilinear stiffness oscillator (Teich, Keilson and Khanna, 1989).

In Figures 1–4, results are shown in the form of (a) displacement waveforms, (b) displacement waveform spectra, (c) velocity waveforms, (d) velocity waveform spectra, and (e) phase-space projections. Figure 1 shows data at $f_s=73$ Hz, below CF; Figure 2 shows data at $f_s=317$ Hz (at CF); Figures 3 and 4 show data at $f_s=610$ and 806 Hz respectively, above CF.

Examining the displacement waveform at the four frequencies indicates that deviations of the waveshape from sinusoidal increase as the signal frequency increases, and is greatest well above CF. The displacement waveforms are more-or-less restricted to the domain of negative displacement for the three higher signal frequencies. This is not the case for the velocity waveforms whose maximal excursions are rather more symmetrical at all signal frequencies. Figures 1 and 3 represent periodic responses; their spectra show only harmonics and/or subharmonics of the signal frequency. The subharmonic resonance evident in Figure 3 is sufficiently strong such that the oscillator is responding maximally at about 300 Hz (near the CF), even though it is being forced at 610 Hz. Figure 2 displays a small number of anharmonic spectral components at frequencies below and above the signal frequency. In contrast, Figure 4 shows abrupt changes in both the displacement and velocity waveforms, resulting in quasi-continuous spectra with many anharmonic components. This behavior suggests the presence of deterministic chaos.

The phase-space projections evidence nonelliptical and asymmetric behavior at all signal frequencies. These distortions from ellipticity increase with increasing signal frequency. The failure of successive cycles to overlap are a manifestation of the anharmonic components of the motion.

The relative magnitudes of the first four velocity harmonics and a subharmonic resonance are shown as a function of signal frequency in Figure 5. These illustrate that the velocity tuning observed at the fundamental frequency is quite different from that observed at the second, third, and fourth harmonics, and from that of the subharmonic

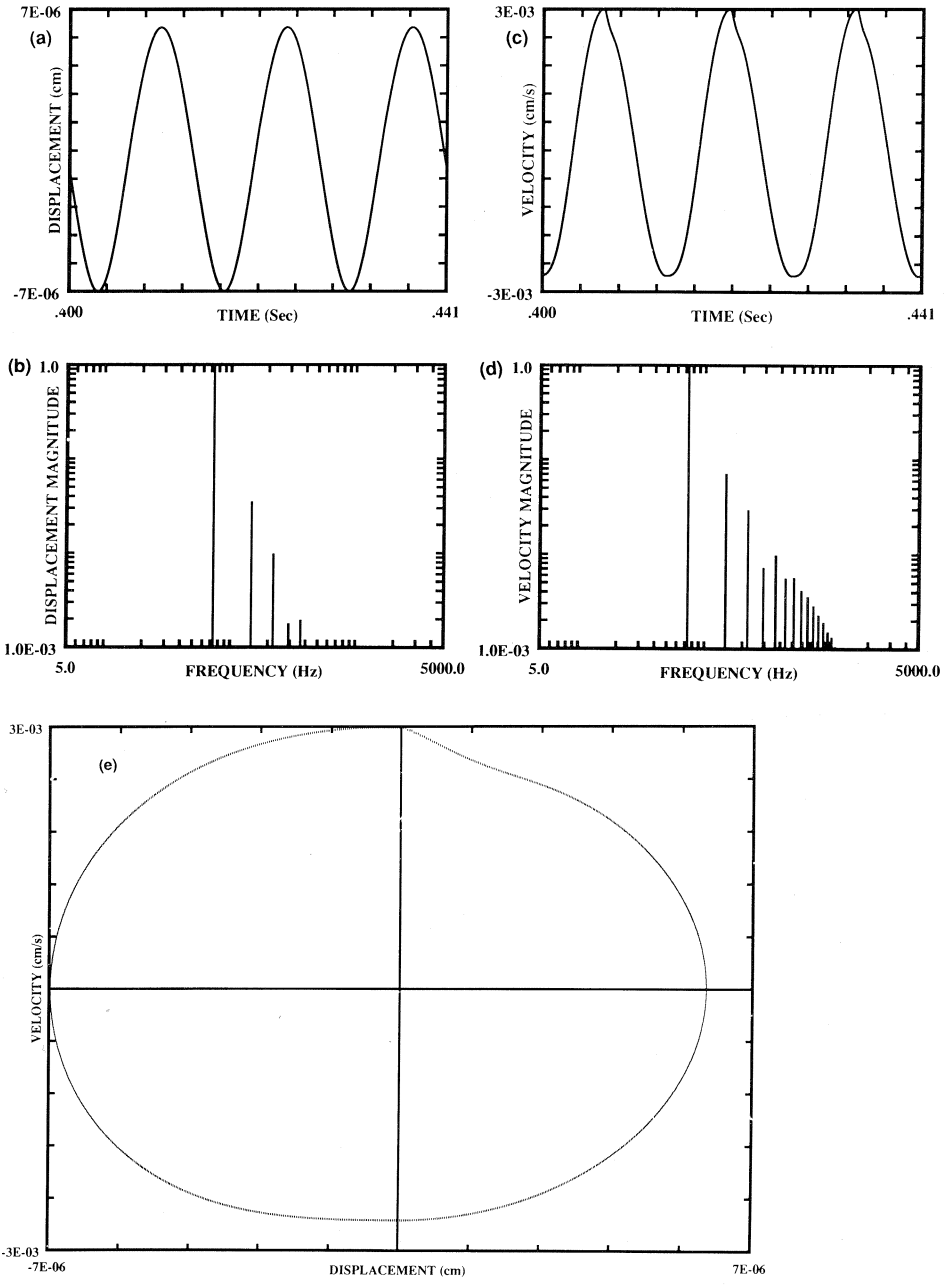

Fig. 1. Response of the bilinear mass oscillator to a signal frequency f_s=73 Hz (below CF). (a) Time waveform of the displacement. The response is quite sinusoidal, but shows a small dc offset toward negative displacements. (b) Fourier spectrum of the displacement waveform. Four harmonics are visible. The ratio of the displacement magnitude at dc (not shown) to the magnitude at the signal frequency is 0.075. (c) Time waveform of the velocity. The waveform deviates most from sinusoidal behavior near its peaks. (d) Fourier spectrum of the velocity waveform. The velocity, being the derivative of the displacement, exhibits a greater number of high-frequency harmonics (12 are visible). (e) Phase-space projection. The trace has an indentation in the upper right quadrant because the distortions of displacement and velocity are phase locked to the positive part of each waveform.

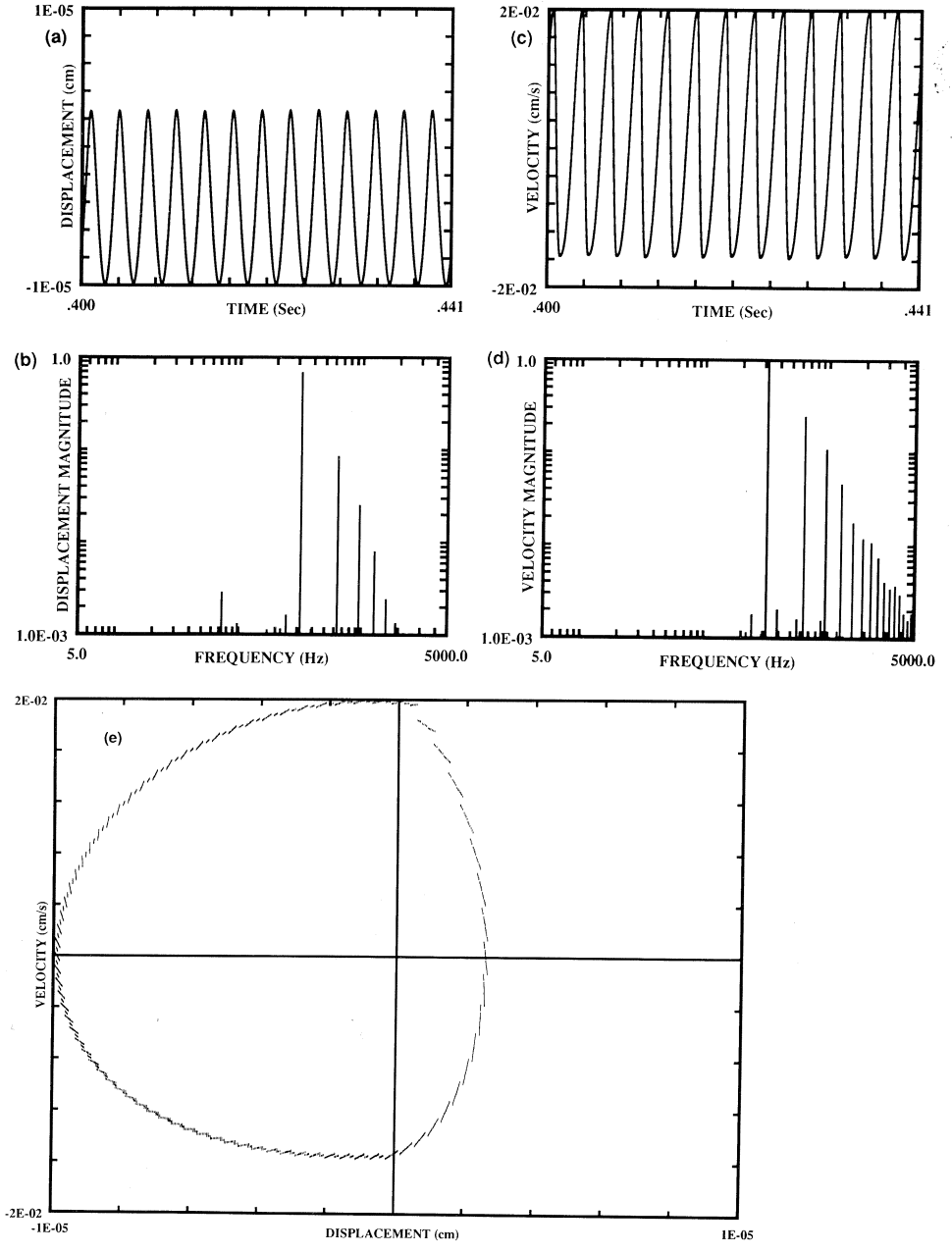

Fig. 2. Response of the bilinear mass oscillator to a signal frequency f_s=317 Hz (at CF). (a) Time waveform of the displacement. The response appears to be quite sinusoidal, but shows a substantial negative dc offset. (b) Fourier spectrum of the displacement waveform; four harmonics are readily seen, of greater relative magnitude than in Figure1(b). There are two anharmonic components visible. The ratio of the displacement magnitude at dc to the magnitude at the signal frequency is 1.45. (c) Time waveform of the velocity. The excursions into domains of positive and negative velocities are unequal. (d) Fourier spectrum of the velocity waveform. Again, a greater number of high-frequency harmonics are seen (about 12) than in the displacement spectrum. There are also a few anharmonic components visible. (e) Phase-space projection. The trace, which is non-elliptical, shows more symmetry for positive and negative velocities than for positive and negative displacements. The trace does not repeat itself. This is a manifestation of the anharmonic components.

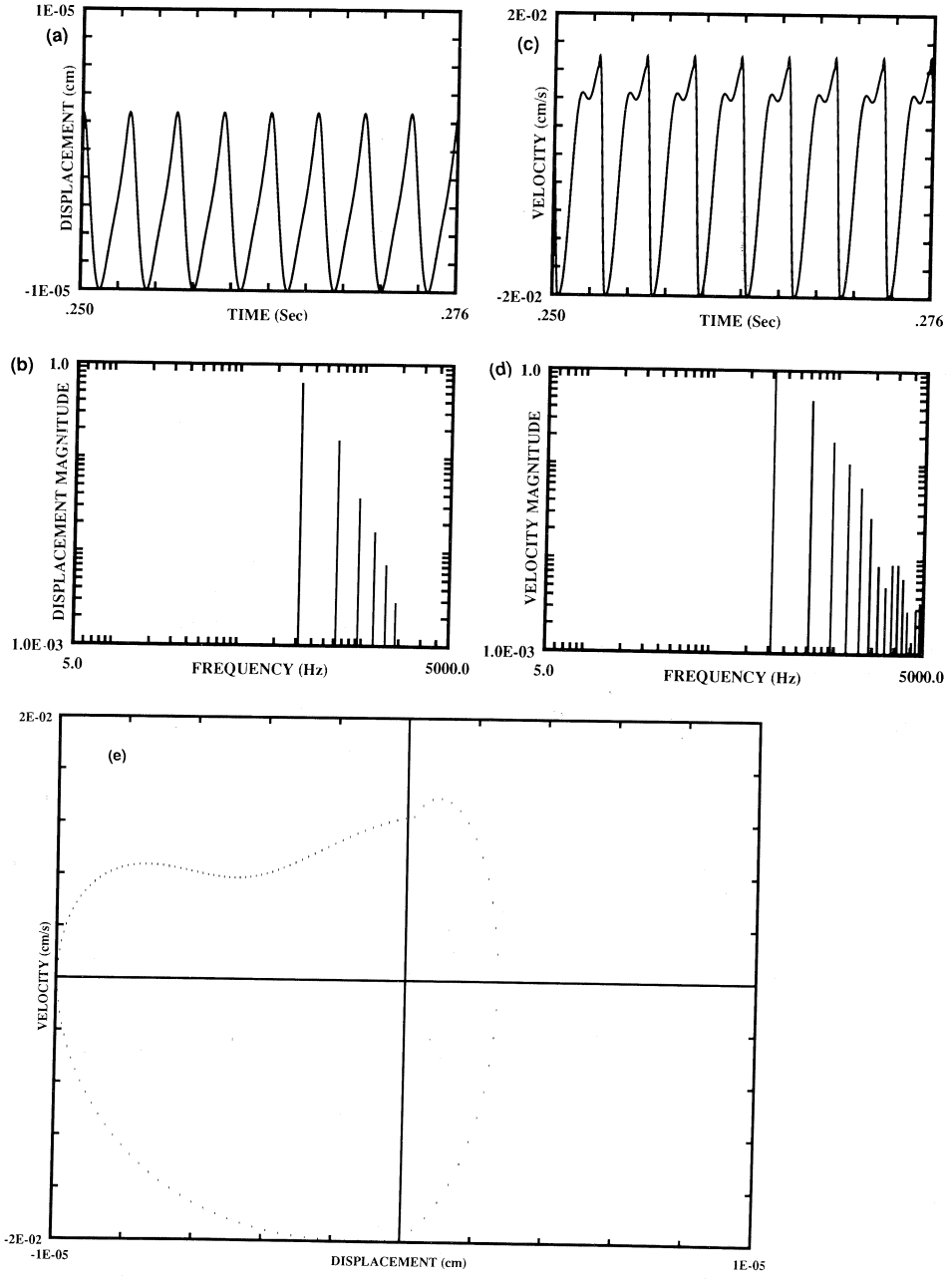

Fig. 3. Response of the bilinear mass oscillator to a signal frequency f_s=610 Hz (above CF). (a) Time waveform of the displacement. The response appears periodic but with a repetition frequency at $f_s/2$. There is also a large negative dc offset. (b) Fourier spectrum of the displacement waveform. Four harmonics of f_s are readily seen, as is a strong spectral component below the signal frequency at about 300 Hz, which is near the CF of the oscillator. This is the subharmonic response. The ratio of the magnitude of the dc component to the magnitude at the signal frequency is 6.47. (c) Time waveform of the velocity. Again, the period of the sinusoidal behavior is twice $1/f_s$ because there is a large response near the CF $\sim f_s/2$. (d) Fourier spectrum of the velocity waveform. More than 10 harmonics are visible. (e) Phase-space projection. The trace is periodic but highly asymmetrical in both velocity and displacement.

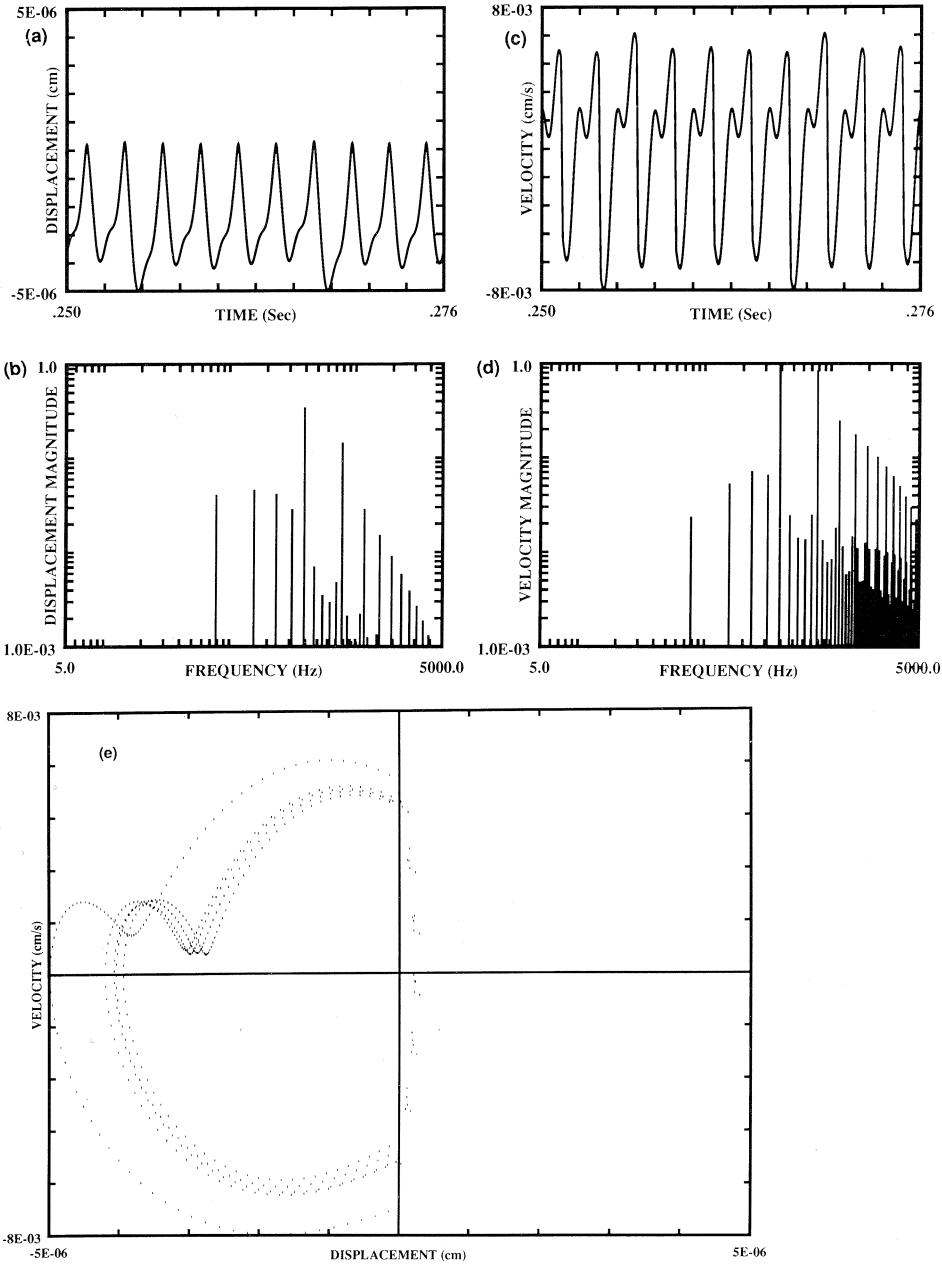

Fig. 4. Response of the bilinear mass oscillator to a signal frequency f_S=806 Hz (well above CF). (a) Time waveform of the displacement. The response has a large negative dc offset which is evidence of rectification. The response shows abrupt changes in the displacement, suggesting the possibility of deterministic chaos. (b) Fourier spectrum of the displacement waveform. Three harmonics of f_s are visible; all of the other components are not multiples of f_s. In addition there are strong spectral components below the signal frequency, with the largest at about 400 Hz. The ratio of the displacement magnitude at dc to the magnitude at the signal frequency is 6.85. (c) Time waveform of the velocity. The response shows abrupt changes in the velocity. (d) Fourier spectrum of the velocity waveform. It shows a quasi-continuum of spectral components which are not harmonics of f_s; this is one of the hallmarks of deterministic chaos. (e) Phase-space projection. The trace first appears to settle on one maximal excursion in velocity and displacement but then abruptly jumps to a larger value. The strong rectification of the displacement is also evident here.

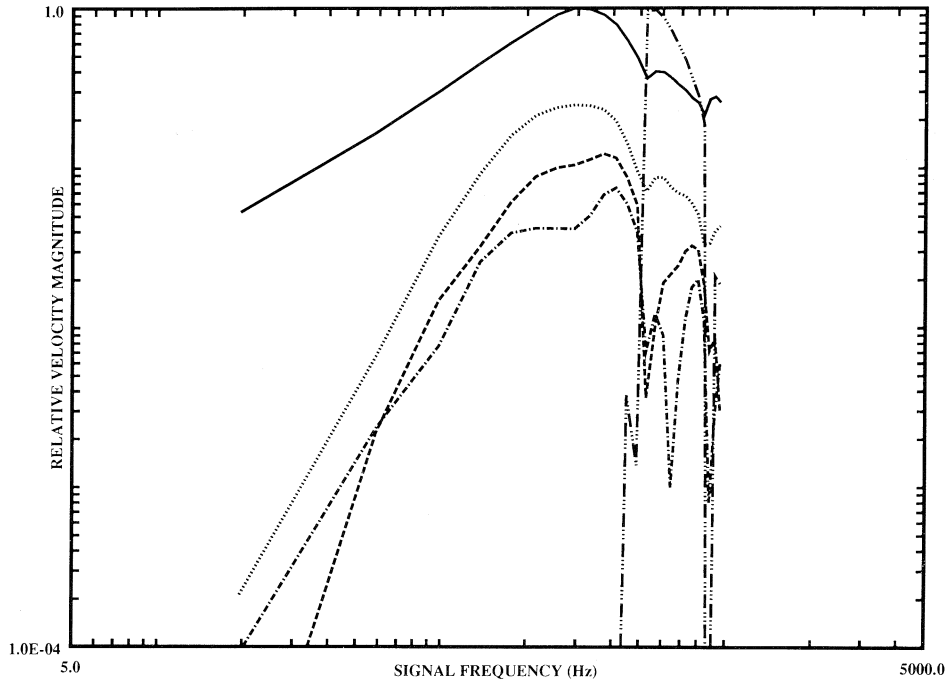

Fig. 5. Relative velocity-magnitude frequency-response curves for the bilinear mass oscillator. The curves represent the magnitude of the first four velocity harmonics, and a sharply tuned subharmonic resonance, plotted as a function of the applied signal frequency. The curves are coded as follows: fundamental (solid curve), 2nd harmonic (dotted curve), 3rd harmonic (dashed curve), 4th harmonic (dash-dot curve), and subharmonic (dash-three-dots curve).

resonance. The frequencies of maximal response (best frequencies) of the third and fourth harmonics lie slightly above that of the fundamental. For this set of parameters, the low frequency slopes of the harmonics are steeper than that of the fundamental. The high frequency tails of all of these curves, including the fundamental, have multiple secondary peaks. The response of the fourth harmonic assumes a highly irregular form at high signal frequencies.

CONCLUSION

For the bilinear mass oscillator model, the number and magnitude of the harmonic components in the displacement and velocity spectra increase with increasing signal frequency. The response shows a sharply tuned subharmonic resonance when the signal frequency is near, but not necessarily precisely at, a multiple of the CF . The relative velocity-magnitude frequency response curves for the first four velocity harmonics all show multiple peaks. The response also exhibits a strong rectification of the waveform and aperiodic distortions at signal frequencies above resonance, suggesting the presence of deterministic chaos.

ACKNOWLEDGEMENTS

This work was supported by the National Institutes of Health and the National Science Foundation.

REFERENCES

Berge P, Pomeau Y, Christian V (1986). Order within chaos. New York: Wiley & Sons.

Keilson SE, Teich MC, Khanna SM (1989). Models of nonlinear vibration. I. Oscillator with bilinear resistance. Acta Otolaryngol (Stockh) Suppl 467: 241–248.

Teich MC, Keilson SE, Khanna SM (1989). Models of nonlinear vibration. II. Oscillator with bilinear stiffness. Acta Otolaryngol (Stockh) Suppl 467: 249–256.

Thompson JMT, Stewart HB (1986). Nonlinear dynamics and chaos. New York: Wiley & Sons.